A statistical regression approach to estimate zooplankton mortality from spatiotemporal survey data

KRISTINA ØIE KVILE[1]*, LEIF C. STIGE[1], IRINA PROKOPCHUK[2] AND ØYSTEIN LANGANGEN[1]*

[1]CENTRE FOR ECOLOGICAL AND EVOLUTIONARY SYNTHESIS (CEES), DEPARTMENT OF BIOSCIENCES, UNIVERSITY OF OSLO, PO BOX 1066 BLINDERN, 0316 OSLO, NORWAY AND [2]KNIPOVICH POLAR RESEARCH INSTITUTE OF MARINE FISHERIES AND OCEANOGRAPHY (PINRO), 6 KNIPOVICH STREET, 183763 MURMANSK, RUSSIA

*CORRESPONDING AUTHOR: k.o.kvile@ibv.uio.no; oystein.langangen@ibv.uio.no

Mortality is notoriously difficult to estimate for zooplankton populations in the open ocean due to the confounding effect of advection. The vertical life table (VLT) approach is commonly used, but has been shown to be sensitive to both spatial and temporal trends in recruitment. Here, we estimate mortality rates of *Calanus finmarchicus* copepodites from spatiotemporally resolved data from the highly advective Norwegian Sea–Barents Sea in spring and summer. We apply both the VLT and a statistical regression approach (SRA), specifically taking into account the effects of advection and spatiotemporal trends in recruitment. Testing the two methods on a simulated dataset shows that the SRA performs better than the most commonly used version of the VLT when trends in recruitment are present. Overall, the SRA appears to be a robust method for spatiotemporally resolved survey data influenced by advection and spatiotemporal trends in recruitment. The estimated mortality rates are relatively low (0.03–0.07 d^{-1}) and indicate increased mortality for the oldest stage pair (copepodites CIV–CV) compared to earlier stages. The results are discussed in the light of previous mortality rate estimates for *C. finmarchicus*.

KEYWORDS: Barents Sea; *Calanus finmarchicus*; copepods; estimation methods; mortality; statistical regression approach; vertical life table; zooplankton

INTRODUCTION

The limited knowledge of mortality rates has been described as one of the main challenges in the modelling of marine population dynamics (Runge *et al.*, 2004). In contrast to attributes such as egg production and growth, which can be estimated by incubating specimens in the lab, mortality is a property of populations and must be determined in the field (Hirst and Kiørboe, 2002). But to estimate mortality rates for zooplankton in the open ocean is challenging due to the influence of advection

(Aksnes and Ohman, 1996). Observing a different number of individuals one day compared to the next can reflect recruitment and mortality, but also transport in or out of the area. Following a zooplankton population in time to estimate mortality (horizontal methods) requires observations from a large enough area to minimise the effect of advection, which is rarely attainable in the open ocean. In addition, the estimation of mortality rates is hindered by spatiotemporal patchiness or bias in observational data, and uncertainty in parameters needed for the estimation (e.g. stage duration) (Ohman, 2012).

As a solution to the confounding effect of advection, Aksnes and Ohman (1996) proposed the vertical life table (VLT) approach. They argued that even in the presence of advection, the composition of zooplankton developmental stages may contain information about mortality and recruitment, assuming different stages are equally influenced by advection and there is no strong trend in cohort structure over time. The VLT has been applied in numerous studies across different systems (e.g. Möllmann, 2002; Plourde *et al.*, 2009a, 2009b; Melle *et al.*, 2014).

Recently, the application of the VLT was criticized for its sensitivity to advection in the presence of spatiotemporal gradients in abundance (Gentleman *et al.*, 2012). In the original article (Aksnes and Ohman, 1996), it was acknowledged that trends in recruitment may bias the mortality estimates, and a framework for correcting this bias was presented. With the exception of some authors testing for trends in egg production before applying the VLT on eggs and naupliar stages (Hirst *et al.*, 2007; Plourde *et al.*, 2009b), the correction framework has received little attention, and other trends in space and time may also affect the mortality estimates (Gentleman *et al.*, 2012). Here, we apply a statistical regression approach (SRA; Langangen *et al.*, 2014), an extension of the VLT that specifically incorporates the role of advection by modelling the effect of space and accounts for trends in time (e.g. recruitment) by inclusion of a seasonal term. By implicitly modelling trends in recruitment, the SRA circumvents the need to remove data potentially violating the VLT's assumptions (e.g. Plourde *et al.*, 2009a). The SRA has previously been applied to estimate mortality of fish eggs (Langangen *et al.*, 2014), and is adapted here and used to estimate mortality in zooplankton populations with variable stage durations and continuous spawning. We apply both the VLT and the SRA to estimate mortality rates of *Calanus finmarchicus* copepodites from long-term, spatiotemporally resolved data from the Norwegian Sea–Barents Sea (NS–BS). In addition, we compare the performance of the two methods on a simulated dataset mimicking the observation data with known mortality rates.

METHOD

The study system

The survey area covers the north-eastern Norwegian Sea and Norwegian continental shelf and south-western Barents Sea (Fig. 1). Mesozooplankton biomass in the area is dominated by *C. finmarchicus*, which typically has an annual life cycle at these latitudes (Eiane and Tande, 2009). Adult stage (CVI) individuals emerge in early spring from overwintering in the deep waters of the Norwegian Sea or fjords (Hirche, 1983; Kaartvedt, 1996; Melle *et al.*, 2004), and spawn in the upper waters. The peak of the spawning period is typically in April–May in the Norwegian Sea (Melle *et al.*, 2004; Broms and Melle, 2007), and occurs progressively later from south-west to north-east into the Barents Sea. The new generation develops from eggs through six naupliar stages (NI–NVI) and five copepodite stages (CI–CV), and in summer [from around mid-June in the Norwegian Sea (Østvedt, 1955)], the older copepodite stages (mainly CV) start to descend for overwintering. The distribution of *C. finmarchicus* in the NS–BS is strongly influenced by advection (Edvardsen *et al.*, 2003; Samuelsen *et al.*, 2009), in particular, the northbound Norwegian Atlantic Current and Norwegian Coastal Current (Blindheim, 2004) (Fig. 1).
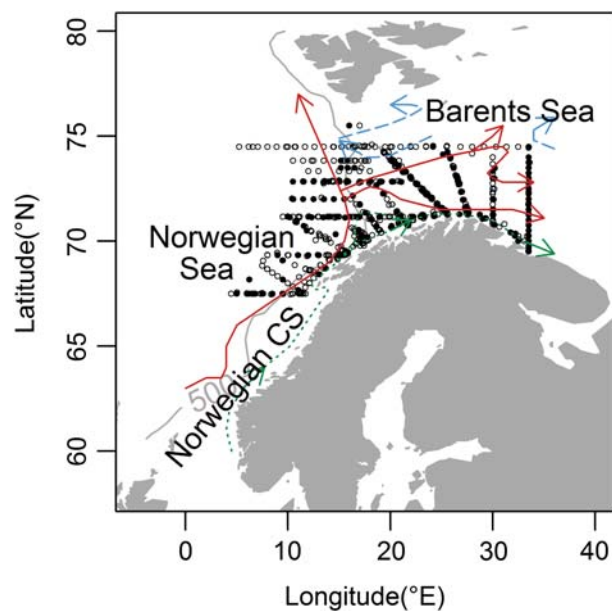

Fig. 1. Study area with survey stations pooled for all years (circles). Filled circles indicate survey stations with available depth-integrated data. The 500 m depth contour (grey line) marks the approximate division between the off-shelf Norwegian Sea and the Barents Sea and Norwegian continental shelf (CS). The main surface currents in the area are indicated (Norwegian Atlantic Current, solid arrows; Norwegian Coastal Current, dotted arrows and Arctic Water Current, dashed arrows).

Mortality estimation

To estimate the instantaneous mortality rate (d^{-1}) of *C. finmarchicus* copepodite stages, we applied the VLT approach (Aksnes and Ohman, 1996) and the SRA (Langangen *et al.*, 2014). Both methods use information about the relative abundance of consecutive developmental stages, and do not require knowledge about absolute abundances. With the VLT, the instantaneous daily mortality rate (m) for the stage pair i and $i + 1$ is the solution to the following equation, where v_i is the abundance of stage i and α_i is the duration of stage i:

$$\frac{v_i}{v_{i+1}} = \frac{e^{(m\alpha_i)} - 1}{1 - e^{(-m\alpha_{i+1})}} \tag{1}$$

It is assumed that the mortality of stage i and $i + 1$ is equal during a period corresponding to the combined duration of the two stages ($\alpha_i + \alpha_{i+1}$). To estimate the mortality rate for adults (q) and the preceding copepodite stage, the corresponding equation is

$$\frac{v_{q-1}}{v_q} = e^{(m\alpha_{q-1})} - 1 \tag{2}$$

Mortality rates are estimated for all data samples separately, and average rates with uncertainty estimates can be calculated given a sufficient number of samples.

The SRA is an extension of the VLT specifically incorporating the effect of advection and varying production. Similarly to the VLT, the SRA estimates average mortality for two consecutive stages. The mortality rate for two consecutive stages is found by estimating the effect of age (in days) on stage-specific abundance using the following generalized additive mixed model (GAMM):

$$\begin{aligned} \ln(N)_{l,t} = {} & \beta_0 + s(spd_l) + te(lon_l, lat_l) + b_{0t} \\ & + (\beta_1 + b_{1t})A_l + \varepsilon_{l,t} \end{aligned} \tag{3}$$

The response variable is the natural log-transformed stage-specific abundance of individuals belonging to stage i or $i + 1$ in station l and year t (zeros excluded). In contrast to the fixed stage durations assumed for fish eggs in the first application of the SRA (Langangen *et al.*, 2014), durations of *C. finmarchicus* developmental stages are known to differ. To account for variable duration of stages i and $i + 1$, abundance is divided by the estimated stage duration. The scaled abundance can be interpreted as the number of individuals of age A (days). The age of individuals of stage i is defined as the midpoint between the day of entry into stage i and into stage $i + 1$ (see "Estimation of development time" section). The covariates include (i) spawning day (*spd*, i.e. the sampling day

minus the estimated age), accounting for seasonal variation in abundance; (ii) sampling position (*lon*, longitude, *lat*, latitude), accounting for spatial variation in abundance and (iii) age (A), accounting for mortality (estimates $-m$). The model includes two random effects: (iv) a random year effect (b_{0t}), accounting for year-to-year variation in total abundance and (v) a random year by age effect (b_{1t}), accounting for year-to-year variation in mortality. β_0 and β_1 are the fixed effects (the intercept and the coefficient of the age effect, respectively), s is a 1D smoothing spline, *te* a 2D tensor product smooth and ε a normally distributed error term.

The model was formulated using the GAM function in the mgcv library in R, treating the random effects as smooths (setting the flag bs = "re") (Wood, 2013; R Development Core Team, 2014). The model code is given in the Supplementary Material, and can be downloaded using the following link: https://github.com/kristokv/SRA. In order to estimate confidence intervals of the mortality estimates from the SRA (the age effect) and the VLT (mean estimate from all samples), we used a non-parametric bootstrap procedure (1000 samples with replacement), with year as the sampling unit (Hastie *et al.*, 2009).

Field data

Stage-specific abundance data of *C. finmarchicus* (ind. m^{-3}) were collected by PINRO (Murmansk, Russia) from 1959 to 1993 in the north-eastern Norwegian Sea and south-western Barents Sea (Fig. 1). Two surveys were conducted per year, in spring (April–May) and summer (June–July). Samples were collected with a Juday plankton net with closing mechanism (37 cm diameter opening, 180 µm mesh size), towed vertically from the lower depth to the upper depth of the sample (Nesterova, 1990). The number of survey stations varied between years, and stage-specific data from both seasons were available from 30 years in total. We did not estimate mortality rates for eggs or naupliar stages, since these are likely undersampled by the mesh size used due to their small size (Hernroth, 1987; Nichols and Thompson, 1991).

Most samples were taken from one of the following depth categories: Upper: upper sampling depth ≤20 m and lower sampling depth ≤60 m (*n*: 3359); Middle: upper sampling depth 40–60 m and lower sampling depth ≤120 m (*n*: 719); Lower: upper sampling depth >90 m (*n*: 721). To avoid bias due to stage-specific vertical distribution patterns, depth-integrated data are typically used for mortality estimation. To ensure a good coverage of the water column when estimating mortality from the survey data, we only included survey stations with samples from all three depth layers (Upper, Middle,

Lower). For these stations, we summed the stage-specific abundances (ind. m^{-3}) from the different depth layers, after multiplying the abundances by the number of metres hauled per layer. This resulted in a total of 504 data points. We also applied the SRA to the full dataset (*n*: 4799). Since around 70% of the samples were from the Upper layer, we first weighted the data to reduce potential bias in the mortality estimates. Depth-specific weights were calculated as 1 divided by the fraction of samples from the respective depth layer (Upper: 0.70, Middle: 0.15, Lower: 0.15), and implemented using the "weights" argument when formulating the GAM.

Simulated data

To test the ability of the two methods to estimate mortality from the type of survey data available, we simulated a *C. finmarchicus* population with known mortality rates, and "sampled" this population to resemble the actual observations. For all years with available survey data, we simulated a population developing from egg-producing females (CVI) in spring to a mix of different developmental stages later in spring and summer. We used an individual-based model with a super-individual (SI) approach (Scheffer *et al.*, 1995), where each SI represents a set of individuals with similar drift history. Each SI initially represents a group of females producing eggs, which in turn develop into copepodites (the egg and naupliar stages are combined) and ultimately new adult females. The initial distribution of SIs was based on modelled evolved overwintering fields in the Norwegian Sea (Hjøllo *et al.*, 2012), focusing on northeastern areas overlapping with the survey area and adjacent areas from where copepods might drift into the survey area (65–72°N, 0–15°E, total number of 4 by 4 km grid cells: 15 346) (Fig. 2). The initial number of adult females in each SI was similarly based on modelled evolved overwintering abundances (Hjøllo *et al.*, 2012), scaled to numbers between 100 and 3300. From this total distribution, we released 3000 randomly selected SIs daily between the 1st and 31st of March each year (in total 93 000 SIs per year).

After release, the SIs are transported passively at 25 m depth using an offline Lagrangian particle-tracking model (Ådlandsvik and Sundby, 1994), with hydrographic forcing from a numerical ocean model hindcast archive (Lien *et al.*, 2013). The archive was constructed with the use of the regional ocean modelling system (ROMS; Shchepetkin and McWilliams, 2005; Haidvogel *et al.*, 2008). The hydrographic information is available for the NS–BS at daily intervals from 1959, with 4 by 4 km horizontal resolution and 32-layer terrain following

vertical resolution. The diffusion coefficient was set at $100 \, \text{m}^2 \, \text{s}^{-1}$.

All adult females in a SI produce eggs at a constant, season-dependent rate. We used observed rates for the Norwegian Sea (Stenevik *et al.*, 2007) for pre-bloom (10 eggs female^{-1} d^{-1}), bloom (22 eggs female^{-1} d^{-1}) and post-bloom (18 eggs female^{-1} d^{-1}) conditions, defining pre-bloom as March–April, bloom as May and post-bloom as June–July. At each time step (day), the stage durations for all stages present in a SI, and the fraction of the total stage durations obtained by that day, are estimated using the ambient temperature at the current position (see "Estimation of development time" section). When individuals complete the duration of a stage, they move to the next. The individuals do not develop beyond the adult stage, thus, a female continues to produce eggs until she dies. At each time step, individuals are removed from the SI according to stage-specific instantaneous mortality rates. We ran the simulation for three different mortality scenarios: (i) stage-specific mortality rates based on previous estimates for *C. finmarchicus* in the Northeast Atlantic (Base) (Melle *et al.*, 2014), (ii) a "High" mortality scenario and (iii) a "Low" mortality scenario (Table I).
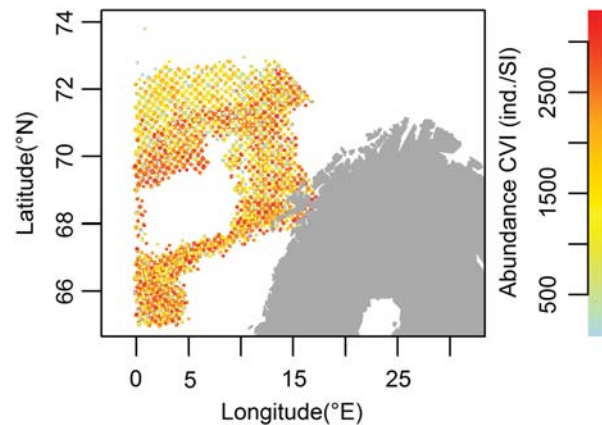

Fig. 2. Initial distribution of simulated SIs and number of adult females (CVI) in each SI, based on evolved overwintering abundances (Hjøllo *et al.*, 2012). From this total distribution, we released 3000 randomly selected SIs daily between the 1st and 31st of March each year.

Table I: Instantaneous mortality rates (d^{-1}) used in the simulations

Scenario	Egg	CI	CII	CIII	CIV	CV	CVI
Base	0.230	0.090	0.105	0.075	0.030	0.025	0.020
High	0.200	0.200	0.200	0.200	0.200	0.200	0.200
Low	0.010	0.010	0.010	0.010	0.010	0.010	0.010

The Base scenario is based on estimates for *C. finmarchicus* in the Northeast Atlantic (Melle *et al.*, 2014).

After drifting for up to 150 days, the SIs were "sampled" at the day and position of actual spring and summer survey stations in the same year (within a 20 km radius). The stage-specific abundances summed from all SIs sampled at the survey stations were used as simulated data for the mortality estimation.

Estimation of development time

We estimated development time (D, in days) from egg to copepodite stage CI, and further for each developmental stage using the Bêlehrádek temperature function fitted for *C. finmarchicus*

$$D = a(T + 10.6)^{-2.05} \quad (4)$$

where T is temperature (°C) and a is a stage-specific constant. Since the ambient temperature estimates for a large fraction of the survey stations (~40%) were below 4°C, we used the coefficients given in Corkett *et al.* (1986) (see "Discussion" section). The function gives the number of days from spawning until a given stage is reached. Stage duration of stage i was calculated as the difference between D for stage i and stage $i + 1$, and the age of stage i as the midpoint between D for stage i and stage $i + 1$. To estimate D during the simulation, we used the ambient temperature estimate from the position of the SI (at 25 m depth), according to the ocean model.

For the observation data, the past temperature experienced by the sampled copepodites is unknown. We therefore assumed D to be a function of temperature at the time and position of the survey station, specifically, the average of the ambient temperature estimates from 10, 50 and 100 m according to the ocean model hindcast archive (Lien *et al.*, 2013). To estimate D for the simulated dataset (after sampling of the SIs), we used the ambient temperature estimates at the time and position of survey stations and the drift depth of the SIs.

Additional analyses

To test the sensitivity of the VLT and the SRA to advection, varying egg production and varying (and unknown) temperature, we constructed three simplified simulated datasets. The simplest (Sim. 1) was a closed population (excluding drift), developing at fixed temperature (5°C) and reproducing at a constant rate (100 eggs per day, independent of the number of females present). This population was sampled at regular intervals after all stages reached stable abundances. The two other datasets (Sim. 2 and 3) were identical to the full simulation (including drift and only sampling SIs present at actual survey stations), but (Sim. 2) setting temperature and egg production fixed or (Sim. 3) setting only temperature fixed. Note that with fixed and known temperature, stage durations and ages of the "sampled" copepodites can be accurately estimated. By adding one level of complexity in each simulation (advection, varying egg production and varying temperature, Table II), and for each added factor comparing the resulting mortality estimates to the results from the preceding simulation (without this factor), we could isolate how each factor influences the mortality rates estimated with the VLT and the SRA.

To calculate realistic confidence intervals of the mortality estimates from the full simulation (Sim. 4), we added random noise with normal distribution and mean zero to the simulated data. The standard deviation of the noise term was calculated as the square root of the difference between the residual variance from the SRA model (Eq. 3) formulated for the actual observation data and for the simulated data. We added this noise to the response variable in the SRA model for the simulated data (on the logarithmic scale), and retransformed to raw data values for the VLT.

RESULTS

Simulated data

Using data from the simplest simulation (Sim. 1), both the VLT and the SRA accurately estimate mortality, with only minor deviations (Table III). When mortality varies between the stages (Base), the estimates for CI–CII are closest to the average value for the two stages, for CII–CIII and CIII–CIV to the true value for the earlier stage, and for CIV–CV to the later stage. As the SRA requires estimates of age and stage duration of both stages in the stage pair, it cannot be used to estimate

Table II: Overview of the different simulation runs used to construct simulated datasets

Sim. no.	Drift	Var. prod.	Var. temp.	Comments
Sim. 1	No	No	No	Closed population developing at 5°C, producing 100 eggs per day
Sim. 2	Yes	No	No	SIs drift according to ocean current hindcasts from the ocean model
Sim. 3	Yes	Yes	No	Egg production depends on month and number of females present in the SIs
Sim. 4	Yes	Yes	Yes	Development depends on ambient temperature hindcasts from the ocean model

Var. prod., varying egg production; var. temp., varying temperature.

Table III: Instantaneous mortality rates (d^{-1}) estimated from the simulated data using the VLT and the SRA (right columns), compared to the true values (left columns)

True mortality				Simulation								
				1. Simple		2. Drift		3. Var. prod.		4. Var. temp.	
Per stage		Mean		VLT	SRA	VLT	SRA	VLT	SRA	VLT	SRA
Base											
CI	0.090	CI–CII	0.098	0.097	0.097	0.100	0.094	0.080	0.090	0.100	0.117
CII	0.105	CII–CIII	0.090	0.101	0.101	0.110	0.098	0.100	0.090	0.110	0.105
CIII	0.075	CIII–CIV	0.053	0.072	0.071	0.090	0.069	0.080	0.070	0.090	0.081
CIV	0.030	CIV–CV	0.028	0.024	0.024	0.070	0.015	0.070	0.010	0.090	0.041
CV	0.025	CV–CVI	0.023	0.015		0.000		0.010		0.020	
CVI	0.020										
High											
CI	0.200	CI–CII	0.200	0.208	0.205	0.210	0.203	0.090	0.190	0.100	0.230
CII	0.200	CII–CIII	0.200	0.216	0.216	0.230	0.214	0.110	0.180	0.120	0.206
CIII	0.200	CIII–CIV	0.200	0.224	0.222	0.240	0.219	0.130	0.190	0.140	0.193
CIV	0.200	CIV–CV	0.200	0.202	0.179	0.240	0.167	0.130	0.150	0.150	0.172
CV	0.200	CV–CVI	0.200	0.212		0.120		0.080		0.100	
CVI	0.200										
Low											
CI	0.010	CI–CII	0.010	0.005	0.005	0.010	0.003	0.060	0.010	0.070	0.041
CII	0.010	CII–CIII	0.010	0.009	0.009	0.020	0.007	0.080	0.010	0.080	0.027
CIII	0.010	CIII–CIV	0.010	0.022	0.022	0.040	0.019	0.120	0.020	0.100	0.020
CIV	0.010	CIV–CV	0.010	0.006	0.006	0.050	−0.002	0.120	−0.010	0.130	0.004
CV	0.010	CV–CVI	0.010	0.029		0.020		0.110		0.140	
CVI	0.010										

Each simulation (1–4) was run for three different sets of mortality rates: Base, Low and High (Table I). See Table S2 (Supplemental Material) for the discrepancies from the true mortality rates in percentage. Var. prod., varying egg production; var. temp., varying temperature.

mortality for CV–CVI (adults). The estimates from the VLT are also less accurate for CV–CVI than the other stage pairs, and we therefore continue focusing on the results for the copepodite stage pairs.

Including drift and sampling at survey stations, but with fixed temperature and egg production (Sim. 2), the VLT tends to overestimate mortality in our dataset, especially for the older stage pairs (CIII–CIV and CIV–CV) (Table III). This is because the stage distributions have not stabilized at the time of the earliest samples in spring; abundances of older stages are still increasing while abundances of younger stages are stable (Fig. S1, Supplementary Material). If only mortality estimates from summer are included in the average, the bias is reduced (Tables S1 and S2, Supplementary Material). Including drift barely influences the SRA estimates compared to the estimates from the simpler simulation (Sim. 1). However, the SRA tends to underestimate mortality for CIV–CV, especially at the High mortality (0.2). At such high-mortality rates, the true age of most sampled copepodites is likely earlier than the midpoint between the two stages. Re-estimating the ages by weighting the days between the two stages by the estimated mortality (e^{-m}) reduces this bias (Tables S1 and S2, Supplementary Material). For the other stages or mortality rates, the difference between the weighted and non-weighted ages is so small that the mortality estimates are barely affected.

When egg production depends on the number of females present in the SIs (Sim. 3), the VLT estimates are more biased, in particular for the High (0.2) or Low (0.01) mortality rates (Table III). At these mortalities, there is a clear decrease (for 0.2) or increase (for 0.01) in abundances with time (Fig. S2, Supplementary Material). As copepodites belonging to the younger of the two stages in the stage pair generally develop slightly before the older (the abundance of the younger stage increase, or decrease, before the older stage), this leads to underestimation of the High mortality and overestimation of the Low mortality. Season-specific estimates are more accurate when the rate of change in abundance is smaller (e.g. for the younger stage pairs in spring at Low mortality) (Tables S1 and S2, Supplementary Material). However, the season-specific VLT estimates are still generally more biased than the SRA estimates. The SRA performs better when data from both seasons are included (Tables S1 and S2, Supplementary Material). As for Sim. 2, the High mortality rate for CIV–CV is underestimated, but improved by weighting the ages by the estimated mortality (Tables S1 and S2, Supplementary Material).

Including varying and unknown temperature (Sim. 4) increases most of the mortality estimates. In spring and summer, temperatures at the sampling stations are generally higher than the ambient temperatures experienced
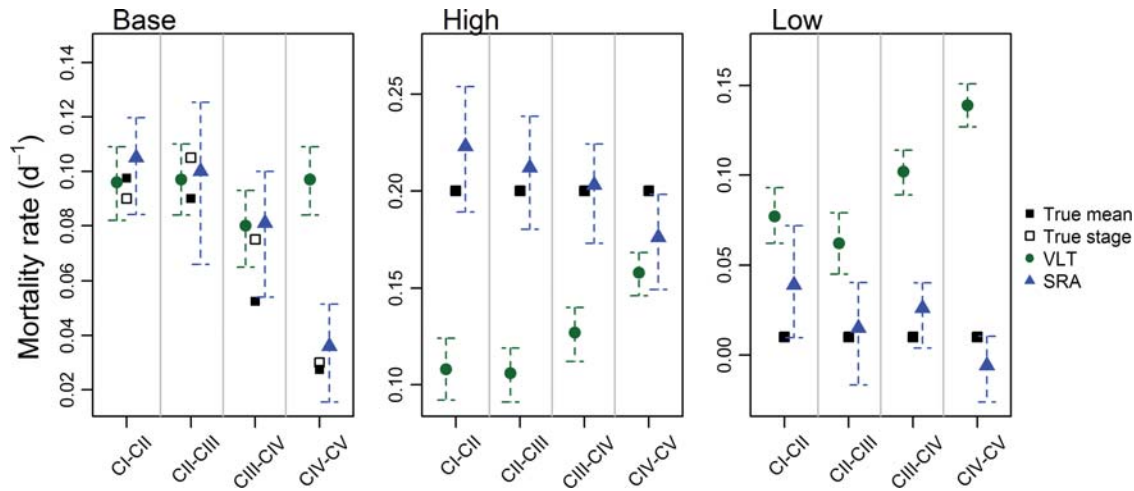
Fig. 3. Estimated mortality rates (d^{-1}) from the VLT (dots) and the SRA (triangles) for data from the full simulation (Sim. 4) with Base, High or Low mortality rates (Table I). In addition to the mean of the true stage-specific mortality rates for each stage pair (filled squares), the true rate for the first of the two stages is plotted for the Base scenario (empty squares). The dashed lines indicate bootstrapped 95% confidence intervals of the estimates. Random noise was added to the simulated data, and the temperature estimates at the sampling stations (used to estimate stage duration after sampling) decreased with 0.7°C.

by the SIs prior to sampling, leading to underestimation of stage duration and overestimation of mortality. A linear regression of temperature by day gave a slope of 0.05°C d^{-1}, which for the earliest stage pair (CI–CII) translates into an increase in 0.7°C from start to end of the duration of the stages combined (on average 14 days), or 1.5°C from spawning to sampling (on average 30 days). Decreasing the temperature estimates at the stations with 0.7°C for the stage duration estimation (a conservative measure for the older stage pairs) reduces the overestimation of mortality rates (Tables S1 and S2, Supplementary Material).

Figure 3 shows the mortality estimates from Sim. 4, with random noise added to the data and the temperature estimates at the stations decreased by 0.7°C. The 95% confidence intervals for both methods are calculated using a bootstrap procedure accounting for spatial autocorrelation. The difference between bootstrapped and nominal confidence intervals was smaller for the VLT than the SRA (mean increase in confidence interval width with bootstrap = 0.003 or 0.01, respectively).

Year-to-year variation in mortality can be estimated with both the VLT (averaging station-specific estimates for 1 year at a time) and the SRA (extracting the random year by age effect from Eq. 3). Interannual mortality estimates for the most realistic simulated dataset (Sim. 4 with added noise), but with the true mortality rate set High (0.2) for the first time period (before 1975) and Low for the last time period (from 1975), show that both methods fail to accurately estimate year-specific mortality, but that the SRA estimates are on average closer to the true rates (Fig. S3, Supplementary Material).

Observational data

For the depth-integrated observational data, the mortality estimates for CI–CII, CII–CIII and CIII–CIV are negative with the VLT and positive with the SRA (Fig. 4). For CIV–CV, the VLT estimates higher mortality than the SRA. Re-calculating the ages in the SRA model by weighting according to the estimated mortality rates increases the estimate for CIV–CV with 0.01. We also applied the SRA on the full dataset, weighting the observations to reduce the influence of bias in the number of samples per depth layer. The estimates from the complete dataset are within the confidence intervals of the depth-integrated data (mean values: CI–CII: 0.03, CII–CIII: 0.03, CIII–CIV: 0.03, CIV–CV: 0.07), but the strong increase in the number of samples (from 504 to 4799) improves the confidence in the estimates (Fig. 4). The estimated interannual standard deviations in mortality from the full dataset ranged from 0.02 to 0.05 d^{-1}, being highest for the younger stages (±standard error: CI–CII: 0.05 ± 0.02, CII–CIII: 0.04 ± 0.01, CIII–CIV: 0.03 ± 0.01, CIV–CV: 0.02 ± 0.01).

For the VLT, ~50% of the station-specific mortality estimates for the three first stage pairs are negative, resulting in overall negative mortality rates. The negative estimates are primarily from summer; if the data are split into season, the estimates from spring are positive (mean values: CI–CII: 0.05, CII–CIII: 0.07, CIII–CIV: 0.11, CIV–CV: 0.16) and the estimates from summer are negative for the first three stage pairs (mean values: CI–CII: −0.09, CII–CIII: −0.12, CIII–CIV: −0.17, CIV–CV: 0.12). Plotting the observed stage-specific
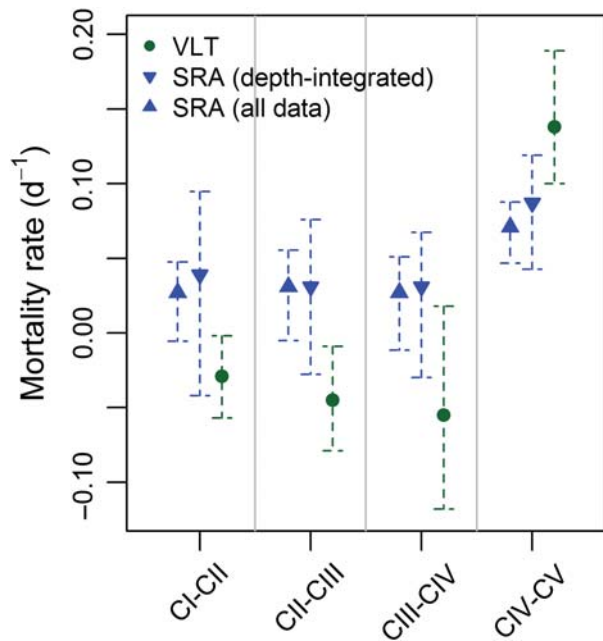
Fig. 4. Estimated mortality rates (d^{-1}) from the VLT (dots) and the SRA (triangles) for the observation data, with bootstrapped 95% confidence intervals of the estimates (dashed lines). The SRA estimates are based on depth-integrated data (point-down triangles, *n*: 504), or all data weighted by depth layer (point-up triangles, *n*: 4799).

abundances by day-of-year shows that CI–CIII generally decrease in summer, CV increases in spring, and both CIV and CV increase in summer (Fig. 5).

DISCUSSION

Performance of the two methods

Recent simulation studies have revealed that mortality rates estimated with the most commonly applied version of VLT (ratio method) are influenced by both temporal trends in recruitment and spatial trends in abundances (e. g. differing stage ratios in upstream vs local areas) (Gentleman *et al.*, 2012). An important assumption of the VLT is that there are no strong trends in recruitment into a particular stage, and while the method is relatively robust to random fluctuations in recruitment, upward or downward trends lead to overestimation or underestimation of mortality, respectively (Aksnes and Ohman, 1996; Gentleman *et al.*, 2012). Our simulation results are in agreement with these findings. For a closed population with stable stage distribution, both the VLT and the SRA were able to capture the true mortality rates. Adding drift did not influence the mortality estimates as long as egg production was uniform in space and time. Adding varying egg production dependent on the number of females present (Sim. 3 and 4) resulted in strong
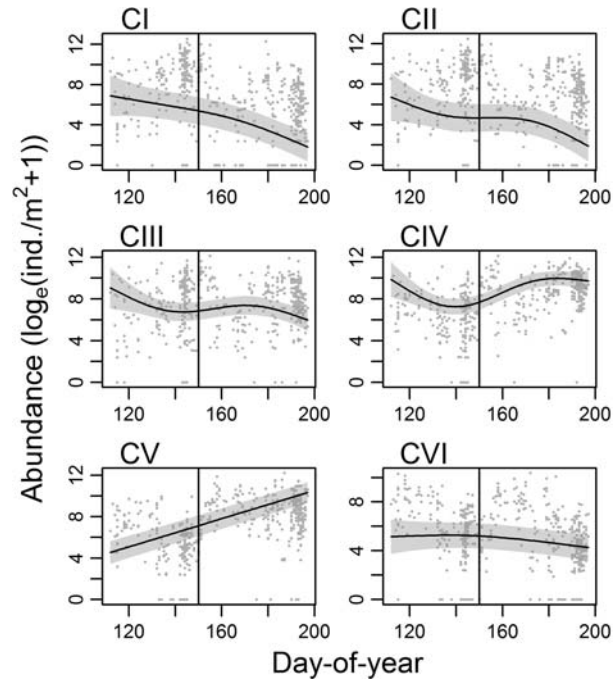

Fig. 5. Stage-specific abundance per day-of-year. The smooth line is the predicted abundance from a GAM of the observation data (natural logarithm of depth-integrated abundance) as a function of sampling position (a two-dimensional tensor product of longitude and latitude) and day (a one-dimensional smooth function of day-of-year). The shaded area is the 95% confidence interval of the predictions, grey dots are actual observations and the vertical line marks the division between the spring and summer survey.

downward trends in recruitment at high mortality, and upward trends at low mortality. In these simulations, the VLT overestimated the low mortality rate and underestimated the high mortality rate. The SRA specifically incorporates temporal variation in abundance through the effect of spawning day, and is therefore more appropriate for data with potential trends in recruitment.

In the actual survey data, abundances of younger stages (CI–CIII) tended to decrease in summer (indicating a downward trend in recruitment of these stages) while abundances of older stages (CIV–CV) tended to increase (indicating an upward trend in recruitment of these stages). According to the simulation results, the VLT should in this situation underestimate mortality for the younger stages, and overestimate mortality for the older stages. The estimated mortality rates were indeed lower (and negative) for the younger stage pairs and higher for the older stage pair (CIV–CV) with the VLT compared to the SRA (Fig. 4), indicating that the observed recruitment trends influenced the VLT estimates in the expected directions.

In their original article, Aksnes and Ohman (1996) provide an analytical expression for how trends in recruitment bias mortality estimates with the VLT (their Eq. 12).

However, using this expression to estimate mortality requires that the trend in recruitment into stage i is known. Difficulties in estimating recruitment trends after the earliest life stages [where egg production may be used (Plourde et al., 2009b)] might explain why this approach has rarely been used. Since potential trends in recruitment are implicitly modelled by the SRA, application of this method might be more straightforward than the corrected VLT.

Various alternative approaches can be used to reduce potential bias resulting from violations of VLT's assumptions. For example, averaging input data in time or space may reduce bias from advection or insufficient sampling (Melle et al., 2014). For our simulated data (Sim. 4 with noise), averaging stage abundances and development time estimates per season and year did not unequivocally improve the results (Table S3, Supplementary Material). Compared to temporal aggregation, aggregating data into spatial subunits might be less straightforward, and is less likely to reduce bias resulting from temporal trends in recruitment.

Unrealistically high or low mortality rates (e.g. >3 or <−1) indicate violation of the assumption of stable recruitment (Gentleman et al., 2012), and are sometimes removed when estimating average mortality (e.g. Heath et al., 2008). However, violations of the VLT's assumptions do not always result in extreme estimates, e.g. no station-specific mortality estimate from our simulated datasets was >3 or <−1. A more rigorous approach is to evaluate if recruitment can be assumed constant, and remove data for which this assumption appears violated. Strong dominance of stage CI or CV–CVI indicates that the population is at the onset of cohort development (Plourde et al., 2009a), as implied in spring for the simulated data with varying egg production and Base mortality (Fig. S4, Supplemental Supplementary Material). The VLT estimates from this simulation were in fact more biased for spring than summer data (Tables S1 and S2, Supplementary Material), but cohort development is not always that obvious (e.g. for the Low mortality, the estimates were also biased, Fig. S4, Supplementary Material). Similarly, to use temporal trends in abundances to highlight periods when the VLT should not be applied (Irigoien et al., 2000) is not always clear-cut (e.g. while abundances of CIII–CIV appear stable in spring in the Low scenario, mortality estimates were biased, Fig. S2, Supplementary Material).

When trends in recruitment were present, the VLT generally performed better with season-specific data, confirming that the method is more appropriate for multiple samples obtained in the same period, reducing additional variability likely present in time series data (Aksnes and Ohman, 1996). The SRA performed better when fitted to data from both seasons. Still, season-specific estimates were generally comparable or closer to the true value than the VLT. It should nevertheless be emphasized that the SRA requires a relatively high density of data. Data from multiple years (ideally more than two, Fig. S5, Supplementary Material) allow the model to separate trends in mortality from seasonal and spatial trends in abundances. If only one season is available, the number of years needed to separate within-year trends in abundances from mortality increases (Fig. S5, Supplementary Material). However, removing the seasonal term ($s(spd_l)$) from the single-season model with data from few years reduces this error (Fig. S6, Supplementary Material). Sufficient spatial sampling is in general necessary to reduce errors in abundance estimates that will propagate to the estimated mortality in ratio methods such as the VLT (Ohman, 2012). Spatially resolved data are also required to let the SRA separate trends in mortality from spatial trends in abundances, and care should be taken when data are spatially limited (and there may not be sufficient data to include the spatial term in the SRA).

A limitation to ratio methods (including the VLT and the SRA) is the uncertainty in estimated stage durations (Ohman, 2012). First, it is assumed that stage durations are equal for all individuals in a sample, while they in reality might vary due to differing environmental conditions prior to sampling. Secondly, the past environment experienced by individuals sampled is unknown, and assumed equal to the survey station. Introducing variable and unknown temperature (Sim. 4) resulted in a bias with both methods, but contrary to the results of Gentleman et al. (2012), the effect of variable stage duration on the VLT estimates was smaller than the effect of trends in recruitment (Sim. 3). This is likely due to changes in egg production being relatively low in the former study, while with the High and Low mortality rates used here, variation in adult female abundance strongly influences egg production. The SRA was more influenced by unknown stage durations than trends in recruitment, but taking into consideration the temperature increase with time reduced the bias with both methods.

Thirdly, we used coefficients for stage duration estimation from Corkett et al. (1986) which cover temperatures below the limits in the study by Campbell et al. (2001). Most studies, also from high-latitude areas, apply the coefficients from the latter study (e.g. Thor et al., 2008; Skardhamar et al., 2011; Dvoretsky and Dvoretsky, 2013), which give shorter stage duration for CI–CIII and longer stage duration for CIV–CV, resulting in higher mortality estimates for the younger stages, and lower for the older stages (Plourde et al., 2009a). For the actual observation data, applying the coefficients from

Campbell *et al.* reduces the (non-significant) differences in estimated mortality with the SRA, giving rates between 0.04 and 0.06 d^{-1} for all stages.

Finally, we considered development to be a function of temperature, assuming excess food supply. We lack information on food availability, but instances of food limitation would result in the stage durations being underestimated, and mortality rates overestimated. Previous studies have however found that doubling the stage durations, a realistic result of food limitation (Campbell *et al.*, 2001), does not influence the estimated mortality rates beyond the range of the confidence intervals presented here (approximately ±0.03) (Ohman *et al.*, 2002; Eiane and Ohman, 2004).

Estimated mortality rates

The simulations indicated that when spatiotemporal data from multiple years are available, the SRA provides more reliable mortality estimates than the VLT. Investigating the actual survey data, we obtained negative estimates with the VLT for the three first stage pairs, indicating violations of the method's assumptions. Neither method provides stage-specific mortality, but rather average mortality for two successive stages, which may introduce errors by smoothing out stage-to-stage variation. However, we believe that this error is relatively small in our analysis of stages CI–CV, as it is expected to mainly affect early stages (Gentleman *et al.*, 2012).

The mortality rates estimated with the SRA were relatively low (0.03–0.07 d^{-1}), but comparable to previous estimates for *C. finmarchicus*, also from the NS–BS region (e.g. Ohman *et al.*, 2004; Dvoretsky and Dvoretsky, 2013) (Table S4, Supplementary Material). Differences between stage pairs were not statistically significant ($P > 0.05$), but indicated higher mortality for CIV–CV. Older (and larger) copepodites may be subject to higher predation pressure by visual predators (Eiane *et al.*, 2002), and stage CV might be more susceptible to food limitation since gonad maturation begins at this stage (Irigoien *et al.*, 2000). Higher estimated mortality of older stages might also reflect vertical overwintering migration of stage CV individuals to depths not covered by the survey (samples from the lower depth category covered on average 85% of the depth layer from ~100 m down to the sea bottom).

Previous studies have also found increased mortality for older stages (CIV–CV or CV–CVI) in the North Atlantic (Irigoien *et al.*, 2000) or Barents Sea (Dvoretsky and Dvoretsky, 2013), while a recent meta-analysis on the contrary indicated higher mortality for early copepodites in the Northeast Atlantic (Melle *et al.*, 2014) (Table S4, Supplementary Material). Results from the Northwest are generally comparable to the Northeast

Atlantic, with the exception of some relatively high mortality rates (>0.2 d^{-1}) estimated for specific areas and seasons (Table S4, Supplementary Material). These studies excluded negative mortality estimates (Plourde *et al.*, 2009a; Pepin, 2013), an approach that should be avoided to obtain unbiased mortality rates when a sufficient number of samples are available (Aksnes and Ohman, 1996). Previous studies using spatiotemporal data from multiple years (e.g. Plourde *et al.*, 2009a; Melle *et al.*, 2014) could have applied the SRA and thereby avoided excluding data (or mortality estimates) potentially violating VLT's assumptions, a practice that may be difficult to perform objectively. When data are limited in space or time, the SRA should be applied with caution, but in these cases, estimates from the VLT might also be biased depending on the state of the population at sampling.

Zooplankton mortality rates are not constant, but influenced by variation in food availability and temperature (Plourde *et al.*, 2009a; Neuheimer *et al.*, 2010), predation pressure (Eiane *et al.*, 2002; Ohman *et al.*, 2008) or infectious agents. Several studies have indicated that zooplankton in the Barents Sea is controlled by predation by capelin, in particular in autumn and in areas to the north and east of our survey area (Hassel *et al.*, 1991; Dalpadado *et al.*, 2012; Stige *et al.*, 2014). Under predation control, we would expect zooplankton mortality to be positively correlated to predator abundance. Due to high uncertainty in the estimates from the simulated data (Fig. S3, Supplementary Material), we did not investigate year-specific mortality rates from the observations. Langangen *et al.* (2014) also found that the SRA did not provide reliable mortality estimates for single years, but the magnitude of the interannual variation was reliably estimated. Our results indicate that interannual variation in *C. finmarchicus* mortality in the NS–BS is higher for early compared to late copepodite stages, but that mortality rates generally remain below 0.1 d^{-1}. Spatial trends in mortality might also be estimated using a modified SRA (by introducing an interaction term between age and location), but this is beyond the scope of this study. Differing mortality rates in space or time can have large impacts on abundances, and should be considered when modelling zooplankton populations.

CONCLUSIONS

The performance of ratio methods such as the VLT is sensitive to processes that affect the abundance ratios between stages (Gentleman *et al.* 2012). We have illustrated how the SRA may correct, at least partly, for

several of the processes that may affect these ratios, including drift between areas with differing stage abundances and temporal trends in egg production. Horizontal methods, like the population surface method (Wood, 1994), follow the progression of a population through successive time points, but demand frequent sampling in time (capturing the full abundance curve) and minimal influence of advection (Aksnes *et al.*, 1997). In our dataset, the same station was generally visited only once or twice per year, and the number of stations sampled varied interannually. Still, the SRA performed well in our most complex simulation, including drift and non-uniform distribution of egg-producing females with continuous spawning. Statistical methods such as the SRA therefore seem a promising tool to acquire knowledge of key population processes such as mortality from non-uniform, spatiotemporal survey data.

SUPPLEMENTARY DATA

Supplementary data can be found online at http://plankt.oxfordjournals.org.

REFERENCES

Ådlandsvik, B. and Sundby, S. (1994) Modelling the transport of cod larvae from the Lofoten area. *ICES Mar Sci. Symp.*, **198**, 379–392.

Aksnes, D. L. and Ohman, M. D. (1996) A vertical life table approach to zooplankton mortality estimation. *Limnol. Oceanogr.*, **41**, 1461–1469.

Aksnes, D. L., Miller, C. B., Ohman, M. D. and Wood, S. N. (1997) Estimation techniques used in studies of copepod population dynamics—a review of underlying assumptions. *Sarsia*, **82**, 279–296.

Blindheim, J. (2004) Oceanography and climate. In Skjoldal, H. R. (ed), *The Norwegian Sea Ecosystem*. Tapir Academic Press, Trondheim, pp. 65–96.

Broms, C. and Melle, W. (2007) Seasonal development of *Calanus finmarchicus* in relation to phytoplankton bloom dynamics in the Norwegian Sea. *Deep Sea Res. Part II Top. Stud. Oceanogr.*, **54**, 2760–2775.

Campbell, R. G., Wagner, M. M., Teegarden, G. J., Boudreau, C. A. and Durbin, E. G. (2001) Growth and development rates of the copepod *Calanus finmarchicus* reared in the laboratory. *Mar. Ecol. Prog. Ser.*, **221**, 161–183.

Corkett, C. J., McLaren, I. A. and Sevigny, J.-M. (1986) The rearing of the marine calanoid copepods *Calanus finmarchicus* (Gunnerus), *C. glacialis* (Jaschnov) and *C. hyperboreus* (Kroyer) with comment on the equiproportional rule. *Syllogeus*, **58**, 539–546.

Dalpadado, P., Ingvaldsen, R. B., Stige, L. C., Bogstad, B., Knutsen, T., Ottersen, G. and Ellertsen, B. (2012) Climate effects on Barents Sea ecosystem dynamics. *ICES J. Mar. Sci.*, **69**, 1303–1316.

Dvoretsky, V. G. and Dvoretsky, A. G. (2013) The mortality levels of two common copepods in the Barents Sea. *Vestn. MGTU*, **16**, 460–465 (in Russian).

Edvardsen, A., Tande, K. S. and Slagstad, D. (2003) The importance of advection on production of *Calanus finmarchicus* in the Atlantic part of the Barents Sea. *Sarsia*, **88**, 261–273.

Eiane, K. and Ohman, M. D. (2004) Stage-specific mortality of *Calanus finmarchicus*, *Pseudocalanus elongatus* and *Oithona similis* on Fladen Ground, North Sea, during a spring bloom. *Mar. Ecol. Prog. Ser.*, **268**, 183–193.

Eiane, K. and Tande, K. S. (2009) Meso and macrozooplankton. In Sakshaug, E., Johnsen, G. and Kovacs, K. (eds), *Ecosystem Barents Sea*. pp. 209–234. Tapir Academic Press, Trondheim.

Eiane, K., Aksnes, D. L., Ohman, M. D., Wood, S. and Martinussen, M. B. (2002) Stage-specific mortality of *Calanus* spp. under different predation regimes. *Limnol. Oceanogr.*, **47**, 636–645.

Gentleman, W. C., Pepin, P. and Doucette, S. (2012) Estimating mortality: clarifying assumptions and sources of uncertainty in vertical methods. *J. Mar. Syst.*, **105–108**, 1–19.

Haidvogel, D. B., Arango, H., Budgell, W. P., Cornuelle, B. D., Curchitser, E., Di Lorenzo, E., Fennel, K., Geyer, W. R. *et al.* (2008) Ocean forecasting in terrain-following coordinates: formulation and skill assessment of the Regional Ocean Modeling System. *J. Comput. Phys.*, **227**, 3595–3624.

Hassel, A., Skjoldal, H. R., Gjøsaeter, H., Loeng, H. and Omli, L. (1991) Impact of grazing from capelin (*Mallotus villosus*) on zooplankton: a case study in the northern Barents Sea in August 1985. *Polar Res.*, **10**, 371–388.

Hastie, T., Tibshirani, R. and Friedman, J. (2009) *The Elements of Statistical Learning: Data Mining, Inference, and Prediction*. 2nd edn. Springer, New York, pp. 249–252.

Heath, M. R., Rasmussen, J., Ahmed, Y., Allen, J., Anderson, C. I. H., Brierley, A. S., Brown, L., Bunker, A. *et al.* (2008) Spatial demography of *Calanus finmarchicus* in the Irminger Sea. *Prog. Oceanogr.*, **76**, 39–88.

Hernroth, L. (1987) Sampling and filtration efficiency of two commonly used plankton nets. A comparative study of the Nansen net and the Unesco WP 2 net. *J. Plankton Res.*, **9**, 719–728.

Hirche, H.-J. (1983) Overwintering of *Calanus finmarchicus* and *Calanus helgolandicus*. *Mar. Ecol. Prog. Ser.*, **11**, 281–290.

Hirst, A. and Kiørboe, T. (2002) Mortality of marine planktonic copepods: global rates and patterns. *Mar. Ecol. Prog. Ser.*, **230**, 195–209.

Hirst, A., Bonnet, D. and Harris, R. (2007) Seasonal dynamics and mortality rates of *Calanus helgolandicus* over two years at a station in the English Channel. *Mar. Ecol. Prog. Ser.*, **340**, 189–205.

Hjøllo, S. S., Huse, G., Skogen, M. D. and Melle, W. (2012) Modelling secondary production in the Norwegian Sea with a fully coupled physical/primary production/individual-based *Calanus finmarchicus* model system. *Mar. Biol. Res.*, **8**, 508–526.

Irigoien, X., Harris, R. P., Head, R. N., Lindley, J. A. and Harbour, D. (2000) Physiology and population structure of *Calanus finmarchicus* (Copepoda: Calanoida) during a Lagrangian tracer release experiment in the North Atlantic. *J. Plankton Res.*, **22**, 205–221.

Kaartvedt, S. (1996) Habitat preference during overwintering and timing of seasonal vertical migration of *Calanus finmarchicus*. *Ophelia*, **44**, 145–156.

Langangen, Ø., Stige, L. C., Yaragina, N. A., Vikebø, F. B., Bogstad, B. and Gusdal, Y. (2014) Egg mortality of northeast Arctic cod (*Gadus morhua*) and haddock (*Melanogrammus aeglefinus*). *ICES J. Mar. Sci.*, **71**, 1129–1136.

Lien, V. S., Gusdal, Y., Albretsen, J., Melsom, A. and Vikebø, F. (2013) Evaluation of a Nordic Seas 4 km numerical ocean model hindcast archive (SVIM), 1960–2011. *Fisk. og Havet*, **7**, 1–80.

Melle, W., Ellertsen, B. and Skjoldal, H. R. (2004) Zooplankton: the link to higher trophic levels. In Skjoldal, H. R. (ed), *The Norwegian Sea Ecosystem*. Tapir Academic Press, Trondheim, pp. 137–202.

Melle, W., Runge, J., Head, E., Plourde, S., Castellani, C., Licandro, P., Pierson, J., Jonasdottir, S. *et al.* (2014) The North Atlantic Ocean as habitat for *Calanus finmarchicus*: environmental factors and life history traits. *Prog. Oceanogr.*, **129**, 244–284.

Möllmann, C. (2002) Population dynamics of calanoid copepods and the implications of their predation by clupeid fish in the Central Baltic Sea. *J. Plankton Res.*, **24**, 959–978.

Nesterova, V. N. (1990) Plankton Biomass Along the Drift Route of Cod Larvae (Reference Material) Murmansk PINRO (in Russian).

Neuheimer, A. B., Gentleman, W. C., Pepin, P. and Head, E. J. H. (2010) Explaining regional variability in copepod recruitment: implications for a changing climate. *Prog. Oceanogr.*, **87**, 94–105.

Nichols, J. H. and Thompson, A. B. (1991) Mesh selection of copepodite and nauplius stages of four calanoid copepod species. *J. Plankton Res.*, **13**, 661–671.

Ohman, M. D. (2012) Estimation of mortality for stage-structured zooplankton populations: What is to be done? *J. Mar. Syst.*, **93**, 4–10.

Ohman, M. D., Runge, J. A., Durbin, E. G., Field, D. B. and Niehoff, B. (2002) On birth and death in the sea. *Hydrobiologia*, **480**, 55–68.

Ohman, M., Eiane, K., Durbin, E., Runge, J. and Hirche, H. (2004) A comparative study of *Calanus finmarchicus* mortality patterns at five localities in the North Atlantic. *ICES J. Mar. Sci.*, **61**, 687–697.

Ohman, M. D., Durbin, E. G., Runge, J. A., Sullivan, B. K. and Field, D. B. (2008) Relationship of predation potential to mortality of *Calanus finmarchicus* on Georges Bank, northwest Atlantic. *Limnol. Oceanogr.*, **53**, 1643–1655.

Østvedt, O. J. (1955) Zooplankton investigations from weather ship M in the Norwegian Sea. 1948–49. *Hvalrådets Skr.*, **40**, 1–93.

Pepin, P. (2013) Distribution and feeding of *Benthosema glaciale* in the western Labrador Sea: fish-zooplankton interaction and the consequence to calanoid copepod populations. *Deep. Res. Part I Oceanogr. Res. Pap.*, **75**, 119–134.

Plourde, S., Pepin, P. and Head, E. J. H. (2009a) Long-term seasonal and spatial patterns in mortality and survival of *Calanus finmarchicus* across the Atlantic Zone Monitoring Programme region, Northwest Atlantic. *ICES J. Mar. Sci.*, **66**, 1942–1958.

Plourde, S., Maps, F. and Joly, P. (2009b) Mortality and survival in early stages control recruitment in *Calanus finmarchicus*. *J. Plankton Res.*, **31**, 371–388.

R Development Core Team (2014) R: a language and environment for statistical computing. *R Found. Stat. Comput. Vienna, Austria* http//www.R-project.org/.

Runge, J. A., Franks, P. S., Gentleman, W. C., Megrey, B. A., Rose, K. A., Werner, F. E. and Zakardijan, B. (2004) Diagnosis and prediction of variability in secondary production and fish recruitment processes: developments in physical-biological modeling. *Sea Glob. Coast. Ocean Multiscale Interdiscip. Process.*, **13**, 413–473.

Samuelsen, A., Huse, G. and Hansen, C. (2009) Shelf recruitment of *Calanus finmarchicus* off the west coast of Norway: role of physical processes and timing of diapause termination. *Mar. Ecol. Prog. Ser.*, **386**, 163–180.

Scheffer, M., Baveco, J. M., Deangelis, D. L., Rose, K. A. and Vannes, E. H. (1995) Super-individuals a simple solution for modeling large populations on an individual basis. *Ecol. Modell.*, **80**, 161–170.

Shchepetkin, A. F. and McWilliams, J. C. (2005) The regional oceanic modeling system (ROMS): a split-explicit, free-surface, topography-following-coordinate oceanic model. *Ocean Model.*, **9**, 347–404.

Skardhamar, J., Reigstad, M., Carroll, J., Eiane, K., Wexels Riser, C. and Slagstad, D. (2011) Effects of mortality changes on biomass and production in *Calanus* spp. populations. *Aquat. Biol.*, **12**, 129–145.

Stenevik, E. K., Melle, W., Gaard, E., Gislason, A., Broms, C. T.Å., Prokopchuk, I. and Ellertsen, B. (2007) Egg production of *Calanus finmarchicus*—a basin-scale study. *Deep Sea Res. Part II Top. Stud. Oceanogr.*, **54**, 2672–2685.

Stige, L. C., Dalpadado, P., Orlova, E., Boulay, A.-C., Durant, J. M., Ottersen, G. and Stenseth, N. C. (2014) Spatiotemporal statistical analyses reveal predator-driven zooplankton fluctuations in the Barents Sea. *Prog. Oceanogr.*, **120**, 243–253.

Thor, P., Nielsen, T. G. and Tiselius, P. (2008) Mortality rates of epipelagic copepods in the post-spring bloom period in Disko Bay, western Greenland. *Mar. Ecol. Prog. Ser.*, **359**, 151–160.

Wood, S. N. N. (1994) Obtaining birth and mortality patterns from structured population trajectories. *Ecol. Monogr.*, **64**, 23–44.

Wood, S. N. (2013) mgcv: GAMs with GCV smoothness estimation and GAMMs by REML/ PQL. R package. Version 1.7–24.